Numerical study of the acoustic properties of micro-perforated panels with tapered hole

Y.J. Qian[a),b)], K. Cui[c)], S.M. Liu[b),d)], Z.B. Li[b),d)], D.Y. Kong[d)] and S.M. Sun[e)]

(Received: 5 December 2013; Revised: 21 May 2014; Accepted: 21 May 2014)

Micro-perforated panel (MPP) absorbers, well known as a basis for the next generation of sound absorbing materials, are now being widely used in noise control engineering. In order to design the structural parameters of MPP absorbers according to the actual demand, a straightforward method to predict the absorption performance of such absorbers is needed. However, traditional predicting methods, such as equivalent electric-acoustic circuit method, the transfer matrix method, modal analysis method and so on, are based on analytical solution. The use of these methods not only requires development and application of special techniques, but also is not suitable for MPPs with irregular-shaped holes, such as tapered holes which can be used to improve the sound absorption performance of a thick MPP absorber. In order to overcome the problem, a numerical procedure based on finite element method (FEM) is developed to obtain the specific acoustic impedance of an MPP. Using this method, the acoustic performance of MPPs with tapered holes as well as the effect of various parameters on their normal incidence absorption performance is numerically investigated and the findings are useful to guide the structural design. © *2014 Institute of Noise Control Engineering.*

Primary subject classification: 35.1; Secondary subject classification: 35.2

1 INTRODUCTION

Micro-perforated panel (MPP) is a thin flat plate perforated with numerous holes of minute dimensions. MPP absorber, well known as a promising basis for the next generation of sound absorbing materials consisting of an MPP fitted in front of a rigid backing wall with an air gap in between, as illustrated in Fig. 1. The acoustic performance of such a device can be completely determined by the hole diameter d, the panel thickness t, the perforation ratio σ, and the depth of the air cavity D[1,2]. Predicting the absorption performance of plane waves impinging on the micro-perforated panel (MPP) is an important technical problem. In fact, such absorbing construction is used widely in various noise control applications such as room acoustics[3], duct mufflers[4], noise barriers[5] and so on. The analysis of MPP absorbers started with Maa using equivalent electrical circuit model. In Maa's MPP model, the panel is assumed to be rigid so that the panel vibration effect is negligible. However, when the panel is flexible or the panel mass per unit area is very small, the panel motion may be significant.

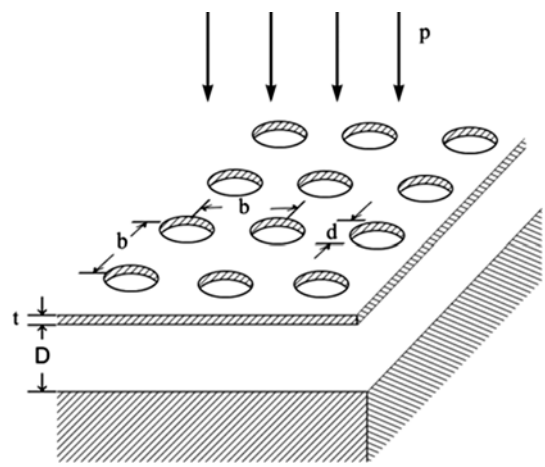

Fig. 1—Schematic diagrams of the MPP absorber.

a) The Internet of Things Engineering College, HoHai University, CHINA; email: qianyujie88@126.com.
b) State Key Laboratory of Transducer Technology, Institute of Intelligent Machines, Chinese Academy of Sciences, Hefei 230031, CHINA.
c) University of Science and Technology of China, Department of Modern Physics, Hefei 230027, CHINA.
d) Department of Automation, University of Science and Technology of China, CHINA.
e) State Key Laboratory of Transducer Technology, Institute of Advanced Manufacturing Technology, Changzhou 213164, CHINA.

Takahashi and Tanaka[6] and Lee et al.[7–9] developed the absorption formula for MPP absorbers based on modal analysis solution of the classical plate equation coupled with the acoustic wave equation which can account for the panel vibration effect. In order to improve the sound absorption performance of traditional single-layer MPP absorbers, multi-layer MPP absorbers were proposed[10,11] and it was found that the transfer matrix method is more convenient than the other approaches to get the absorption coefficients[12].

However, most of the studies mentioned above on sound absorption performance of MPP absorbers are done using analytical methods. The use of these methods not only requires development and application of special techniques, but also is not applicable for MPPs with irregular-shaped holes, such as tapered holes which can be used to improve the sound absorption performance of a thick MPP absorber[13]. This obvious disadvantage of analytical methods restricts thereby their use to MPPs with perforations of few simple shapes, such as cylindrical holes, square holes and rectangular holes[14]. On the contrary, numerical methods have been found to be efficient and versatile in modeling the acoustic characteristics of various acoustic materials and acoustic structures. Achenbach used the boundary element method to study the three-dimensional reflection and transmission of a plane acoustic wave by a grating composed of parallel equidistant rods[15]. Liu and Herrin[16] also conducted a boundary element analysis to simulate the effect of the mico-slit absorber (MSA) and adjoining cavity with and without partitioning on the sound field in the plenum. The results showed that the simulation agreed well with experimental data when it was assumed that the MSA could be modeled via a transfer impedance boundary condition. Easwaran and Munjal[17] presented a finite element scheme based on the Galerkin technique to analyze the reflection characteristics of a resonant absorber when insonified by a normal incidence plane wave. Onen[18] studied the absorption properties of MPP absorbers made from the commercial composite material Parabeam with micro diameter holes drilled on one side based on finite element model, but the acoustic impedance of MPP is calculated in advance using analytical methods in their models, and only the acoustic impedance of the cavity with fibrous materials is obtained by the finite element method (FEM); therefore, they cannot handle MPPs with irregular-shaped holes. It is generally known that most of the acoustic FEM softwares already include porous materials models but perforated systems require specific formulations. Addressing this problem, Atalla and Sgard[19] found that rigid perforated plates and screens may be modeled as rigid porous materials by selecting appropriate parameters and then the acoustic performance of MPP absorbers can be obtained with the help of the acoustic software based on finite element analysis or transfer matrix method. It has been shown that using this method, either rigid[20] or flexible arbitrarily-shaped micro-perforated panels[21] could be modeled using finite element methods. Moreover, Randeberg has applied some numerical methods to calculate the normal incidence absorption coefficients of MPPs with horn-shaped orifices, but the experimental data shows that the numerical models presented by Randeberg[22] are not precise enough to predict the sound absorption performance of MPP absorbers. Recently, it has also been shown that the techniques of computational fluid dynamics (CFD) can be used to calculate the transfer impedance of rigid micro-perforated panels with cylindrical holes[23] or tapered holes[24]. However, the air flow in the CFD model is assumed to be incompressible which is not according with the true condition and may result in an underestimate of energy loss in the holes. Additionally, the motion of air flow in the hole is solved in the time domain in the CFD model, and the velocity and pressure obtained need to be transformed from time domain to frequency domain through Fourier transforms, which will increase the complexity.

In this study, in order to accurately predict the normal incidence absorption performance of an MPP with tapered holes, an alternative approach based on FEM has been presented. Especially, the emphasis has been placed on the acoustic impedance of the single hole, since the modeling of a single hole can take into account the hole shapes which makes it suited to MPPs with irregular-shaped holes. Furthermore, in our finite element model, the air flow is modeled as viscous and thermally conducting, compressible fluid which makes the model built more in line with the actual situation. The contents in this paper are arranged as follows except the introduction given in the current section. Maa's model of an MPP absorber is briefly introduced in Sec. 2 which will help to understand the finite element analysis method used in this study. Then, a finite element modeling procedure of a single cylindrical hole as well as a tapered hole is established in Sec. 3. In Sec. 4, the present model of the cylindrical hole MPP and the tapered hole MPP is validated against experimental results. In what follows, Sec. 5 conducts a theoretical parameter study to investigate the impact of each of these three parameters (such as the hole inlet diameter, the hole outlet diameter and the panel thickness) on the normal incidence absorption performance of MPP absorbers with tapered holes. Section 6 is the concluding remarks about this study. Finally, it is worth noting that the whole study is based on the assumption that the MPP is rigid and thus the panel vibration effect can be neglected.

2 MAA'S MODEL

Maa's model of an MPP absorber was first put forward in 1975, and simplified later, to allow the acoustic properties of an MPP absorber to be precisely predicted[1]. Maa's calculation formula of absorption coefficients is deduced from Rayleigh's formulation for wave propagation in narrow tubes[25]. Based on these equations, Crandall modeled dissipation in small cylindrical tubes[26], and Maa further developed Crandall's model for the case of very small holes in which the viscous boundary layer spans the whole hole. For a cylindrical hole model, assuming the sound pressure difference between the two ends of the hole to be Δp, the equation for its normal specific acoustic impedance is expressed as:

$$z_h = \frac{\Delta p}{\bar{u}} = \frac{32\rho\mu t}{d^2}\sqrt{1+\frac{k^2}{32}} + j\omega\rho t\left(1+\frac{1}{\sqrt{3^2+\frac{k^2}{2}}}\right), \quad (1)$$

with

$$k = \sqrt{\frac{\rho\omega}{\eta}}\frac{d}{2} = \sqrt{\frac{\omega}{\mu}}\frac{d}{2}, \quad (2)$$

where $\bar{u}$ is the average axial velocity of air in the tube, t is the panel thickness, d is the diameter of the tube, η is the dynamic viscosity constant of air, ρ is the air density, $\mu = \eta/\rho$ is the kinematic viscosity constant of air, $\omega = 2\pi f$ is the angular frequency of incident acoustic wave, and $j = \sqrt{-1}$ is the unit imaginary number. The normal specific acoustic transfer impedance of an MPP (plus end correction) can be given as:

$$Z_M = \frac{1}{\sigma}\left(\frac{32\rho\mu t}{d^2}\sqrt{1+\frac{k^2}{32}} + j\omega\rho t\left(1+\frac{1}{\sqrt{3^2+\frac{k^2}{2}}}\right)\right) + \frac{2\sqrt{2\omega\rho\eta}}{\sigma} + \frac{j0.85\omega\rho d}{\sigma}, \quad (3)$$

where σ is the perforation ratio (total area of the perforation on a unit area of panel). The first term in Eqn. (3) corresponds to the internal impedance of the holes. The second term is the viscous end correction, which accounts for the dissipative effects occurring in the panel surface near the holes. The last term is the mass-end correction corresponding to the mass of air moving around the opening of the holes. Total surface normal impedance of the MPP layer is simply the sum of acoustic impedance of the air cavity Z_D and MPP Z_M:

$$Z_{\text{total}} = Z_M + Z_D, \quad (4)$$

with

$$Z_D = -j\rho c\cot(\omega D/c), \quad (5)$$

where D is the depth of the cavity. The resulting normal incidence sound absorption coefficient α can be calculated as:

$$\alpha = 1 - \left|\frac{Z_{\text{total}} - \rho c}{Z_{\text{total}} + \rho c}\right|^2. \quad (6)$$

3 FINITE ELEMENT MODEL OF A SINGLE HOLE

3.1 Cylindrical Hole

A 2D acoustic FEM approach, the acoustic module in COMSOL Multiphysics which has been widely applied in simulation for fan noise control using micro-perforated panels[27,28], is used to calculate the specific acoustic impedance of a single hole by defining proper boundary and interface conditions. The model was made axisymmetric to make the calculation time relatively short. Figure 2(a) shows the cylindrical hole model. Note that the axis for this axisymmetric geometry is at the left of the sketch. Assuming a viscous and thermally conducting, compressible flow, its motion is governed by the following set of equations listed in Eqn. (7)[29]:

$$\begin{cases} i\omega\rho_0\mathbf{u} = \nabla\cdot\left[-p\mathbf{I}+\mu(\nabla\mathbf{u}+(\nabla\mathbf{u}))^T-\left(\frac{2}{3}\mu-\mu_B\right)(\nabla\cdot\mathbf{u})\mathbf{I}\right] \\ i\omega\left(p\frac{\partial\rho_0}{\partial p}+\frac{\partial\rho_0}{\partial T}\right)+\rho_0\nabla\cdot\mathbf{u}=0 \\ i\omega\rho_0 C_P T = -\nabla\cdot(-k\nabla T) - i\omega p\frac{T_0}{\rho_0}\frac{\partial\rho_0}{\partial T} \end{cases} \quad (7)$$

where the first equation is the momentum equation (the Navier–Stokes equation), the second is the continuity

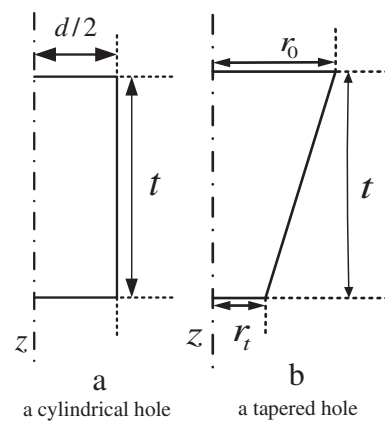

Fig. 2—Cross-sectional view of a single hole model.

equation and the third is the energy equation formulated using the Fourier heat law. In Eqn. (7), the dependent variables are pressure p, velocity $\mathbf{u}$, temperature T, and density ρ_0; k is thermal conductivity; μ is the dynamic viscosity and describes losses due to shear friction; the coefficient μ_B is the bulk viscosity and describes losses due to compressibility (expansion and contraction of the fluid); C_P is the specific heat at constant pressure; $\mathbf{I}$ is the unit vector. The boundary conditions used in this paper are sound-hard boundaries, and there is no slip of the viscous flow:

$$\mathbf{u}_b = 0. \tag{8}$$

where $\mathbf{u}_b$ describes the velocity on the boundary. The mesh size used in this model is physically controlled to be extremely fine (the finest grid size in COMSOL Multiphysics) and there are 5678 mesh elements and 7984 nodes, as can be seen in Fig. 3(a). The boundary condition at the inlet involves a combination of an incoming (amplitude 0.1, to ensure that the velocity is low enough to avoid non-linear effects[30]) and outgoing plane wave parallel to the flow or z direction (see Fig. 2). At the outlet boundary, the model specifies an outgoing plane wave. The outputs of the COMSOL Multiphysics simulation are the complex pressure and the axial complex velocity at each node. For a cylindrical hole of constant diameter, the average speed of each cross section is equivalent. Thus only the inlet velocity of each node is required and the average axial velocity over the tube cross-section can be given by:

$$v = \frac{1}{\pi {r_0}^2} \sum_{m=1}^{M} 2\pi r_m v_m \Delta r_m. \tag{9}$$

Here r_m is the radial length of element m, r_0 is the radius of the inlet section, Δr_m is the radial distance between element m and element $m-1$, v_m denotes the axial velocity of element m, and M is the total number of elements in the cross section. The specific acoustic impedance of the hole is calculated as:

$$z_h = (p_2 - p_1)/\overrightarrow{v}. \tag{10}$$

Here, p_1 denotes the inlet pressure and p_2 is the outlet pressure. The acoustic impedance of an MPP absorber is then, with the addition of the acoustic impedance of the cavity and end corrections,

$$Z_{\text{total}} = \frac{z_h}{\sigma} + \frac{2\sqrt{2\omega\rho\eta}}{\sigma} + \frac{j0.85\omega\rho d}{\sigma} - j\rho c \cot(\omega D/c). \tag{11}$$

The normal incidence absorption coefficient for the absorber can be calculated by Eqn. (6) as before.

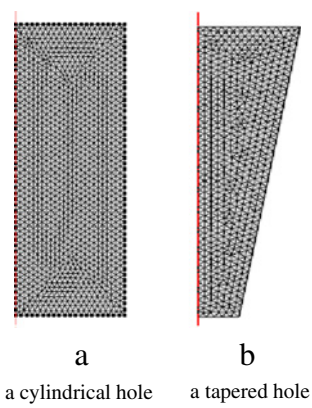

Fig. 3—Typical computational mesh in the region of the perforation.

3.2 Tapered Hole

The tapered hole model is also made axisymmetric to make the time short, as illustrated in Fig. 2(b). The equations of the problem solved and the boundary conditions for the tapered hole model are set the same as the cylindrical hole model. The mesh size is also physically controlled to be extremely fine and there are 4426 mesh elements and 5986 nodes, as can be seen in Fig. 3(b). Since the average speed of each cross section is unequal, the tapered hole is divided into N short tapered shells, and each tapered shell can be equivalent to a cylindrical tube of length $\Delta z = t/N$ if Δz is small enough. The acoustic impedance of each of these short tubes is calculated according to the cylindrical hole model and then added, and the result is the total acoustic impedance of the tapered hole:

$$z_h = \sum_{n=1}^{N} \frac{p_{n,2} - p_{n,1}}{\overrightarrow{v_n}}. \tag{12}$$

Here, the complex pressure at the front side and rear side of shell n are denoted as $p_{n,1}$ and $p_{n,2}$, respectively. $\overrightarrow{v_n}$ denotes the average velocity at the front side of shell n, which is also calculated by Eqn. (9). The acoustic impedance of the tapered hole panel absorber is then calculated as:

$$Z_{\text{total}} = \frac{z_h}{\sigma} - j\rho c \cot(\omega D/c). \tag{13}$$

End corrections can in fact be neglected in this case since the tapered hole is often used to enhance the absorption performance of thick panel absorbers which results in low value of d/t (see Ref. 1). The normal incidence absorption coefficient for the absorber is also evaluated with the aid of Eqn. (6).

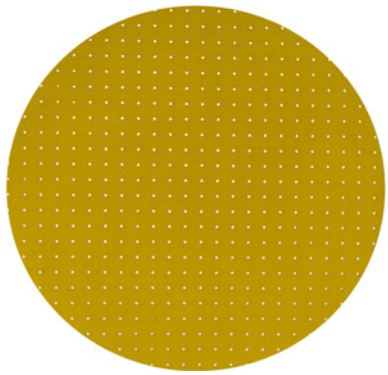

Fig. 4—Photograph of epoxy MPP.

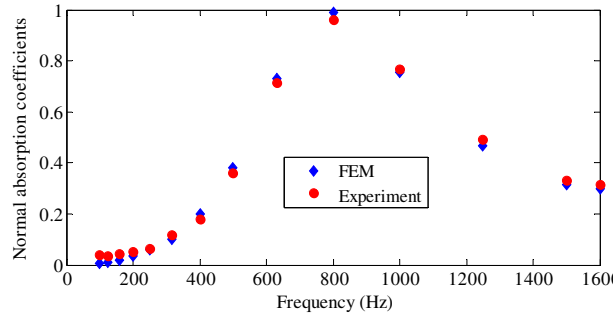

Fig. 6—Comparison of normal incidence absorption coefficient of sample No. 1.

4 MODEL VALIDATION

As a preliminary validation of the finite element modeling procedure, the normal incidence sound absorption characteristics of two MPP absorbers with cylindrical holes are simulated and compared with experimental data obtained in impedance tube using standing wave ratio method[31]. The first numerical example, namely sample No. 1, consists of an MPP with relatively big holes (the hole diameter is usually larger than 100 μm) fitted in front of a solid wall with a constant air gap of $D = 30$ mm. Other structural parameters of the MPP are $d = 0.5$ mm, $t = 2$ mm, $\sigma = 1.92\%$. The second numerical example, namely sample No. 2, is made of an MPP with ultra-micro perforations (the hole diameter is smaller than 100 μm) together with an air cavity of $D = 20$ mm behind it. The other structural parameters are $d = 0.044$ mm, $t = 0.2$ mm, $\sigma = 13.53\%$. Sample No. 1 is made out of epoxy resin through the use of mechanical punching, as shown in Fig. 4. MEMS technology is applied to fabricate sample No. 2 using silicon chip, as shown Fig. 5. Both of the panels are rigid enough to neglect the effect of panel vibration. The simulation and measurement of the normal incidence absorption coefficients for sample No. 1 are carried out in 1/3 octave-band center frequencies between 100 and 1600 Hz in the impedance tube with 100 mm in diameter. Similarly, the simulation and measurement of normal incidence absorption coefficients for sample No. 2 are carried out in 1/3 octave-band center frequencies between 1500 and 6000 Hz using the impedance tube with 29.6 mm in diameter. The results obtained experimentally and by using FEM are compared in Figs. 6 and 7, respectively. It can be seen from Figs. 6 and 7 that the FEM results agree well with experimental results.

Finally, the normal incidence absorption coefficients for MPP absorbers with tapered holes calculated by using FEM are compared with the experimental results available in Ref. 13. The structure parameters are shown in Table 1, where $d1$ is the hole inlet diameter at the sound incident side, $d2$ is the hole outlet diameter at the back side, t is the panel thickness, b is the distance between hole center (all of them are measured in mm), and σ is the perforation ratio (usually in % and based on the hole inlet diameter). The comparison result is plotted in Fig. 8, where it can be seen that the numerical results compare well with the experimental results. Slight differences between the curves may be due to small manufacturing imperfections (see Ref. 13) of the panels and their positioning inside the tube or the neglect of the end correction.

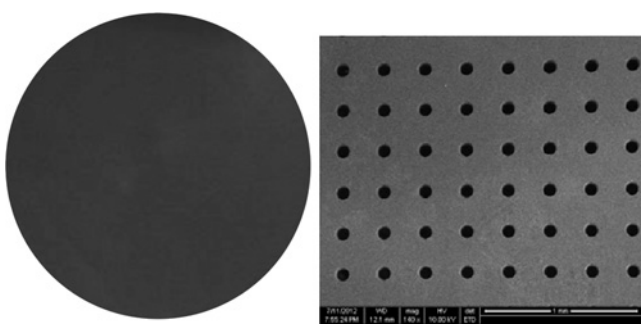

Fig. 5—Photograph and SEM micrograph of silicon MPP.

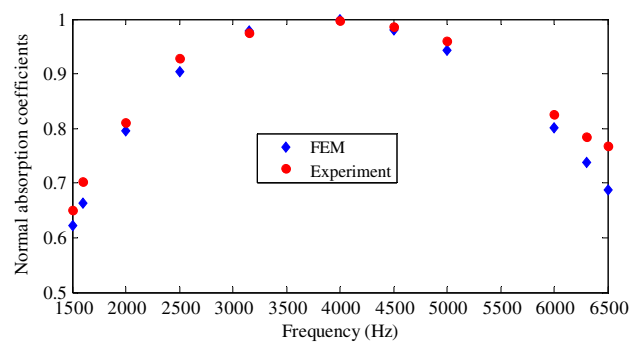

Fig. 7—Comparison of normal incidence absorption coefficient of sample No. 2.

Table 1—Structure parameters of an MPP absorber with tapered holes.

Structural parameters	*t* (mm)	*d1* (mm)	*d2* (mm)	*b* (mm)	*σ* (%)	*D* (mm)
Tapered hole MPP	10	0.5	0.8	5	0.79	56

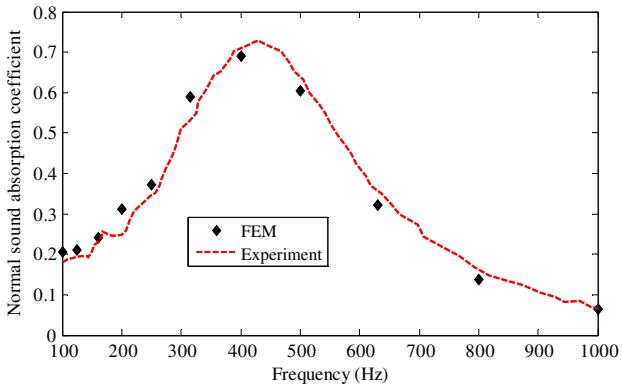

Fig. 8—Comparison of normal incidence absorption coefficient of MPP absorber with tapered holes.

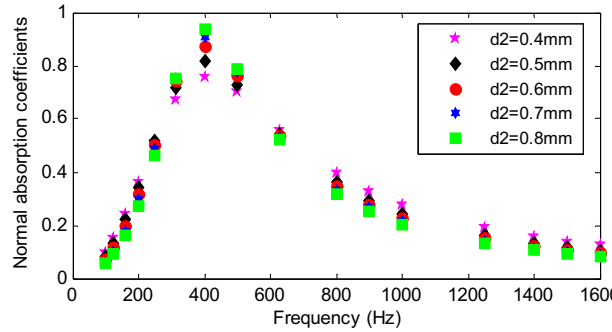

Fig. 9—Normal incidence absorption coefficient of Set 1 MPP absorbers.

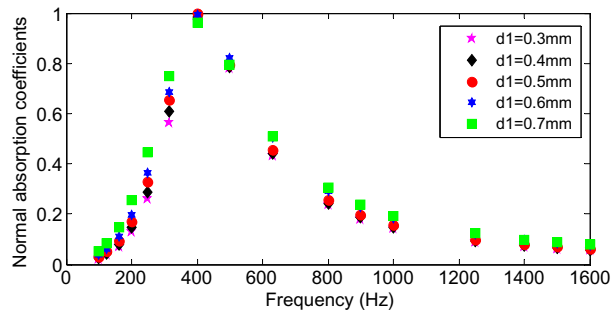

Fig. 10—Normal incidence absorption coefficient of Set 2 MPP absorbers.

5 NUMERICAL RESULTS AND FINDINGS

The acoustic properties of the tapered hole MPP absorbers are investigated numerically using the finite element procedure presented above. There is no optimization procedure behind the chosen dimensions for parameters. Three sets of models were considered in which the following parameters were changed: the hole outlet diameter, the hole inlet diameter and the panel thickness. The cavity depth is kept constant at 30 mm under all conditions. The specific parameters for the three sets of models are listed in Table 2. Note that in Table 2, *d*1, *d*2, *t*, *b*, *σ*, and *D* have the same meaning and units as those in Table 1. Numerical results based on finite element method are shown in Figs. 9, 10 and 11, respectively. It can be seen from Fig. 9 (set 1) that with the hole inlet diameter remaining unchanged, the absorption peak value increases as the hole outlet diameter increases, and the absorption bandwidth tends to become narrow. This may be because the increase of the hole outlet diameter results in the slightly increasing acoustic mass of the MPP when the hole outlet diameter remains the same, and in the meanwhile makes its acoustic resistance match the acoustic resistance of air better. Figure 10 (set 2) indicates that when the hole size of the inlet side increases, the maximum absorption coefficient gradually decreases, but the absorption

Table 2—Structural parameters of three model sets.

Set 1: Hole outlet diameter				Set 2: Hole inlet diameter					Set 3: Panel thickness					
d1	*σ*	*t*	*b*	*d2*	*d2*	*t*	*b*	*σ*	*d1*	*d1*	*d2*	*b*	*σ*	*t*
0.3	1.77	8	2	0.4	0.9	8	4.5	0.35	0.3	0.4	0.8	4	0.785	4
0.3	1.13	8	2.5	0.5	0.9	8	4.5	0.62	0.4	0.4	0.8	4	0.785	5
0.3	0.76	8	3	0.6	0.9	8	4.5	0.97	0.5	0.4	0.8	4	0.785	6
0.3	0.58	8	3.5	0.7	0.9	8	4.5	1.39	0.6	0.4	0.8	4	0.785	7
0.3	0.44	8	4	0.8	0.9	8	4.5	1.89	0.7	0.4	0.8	4	0.785	8

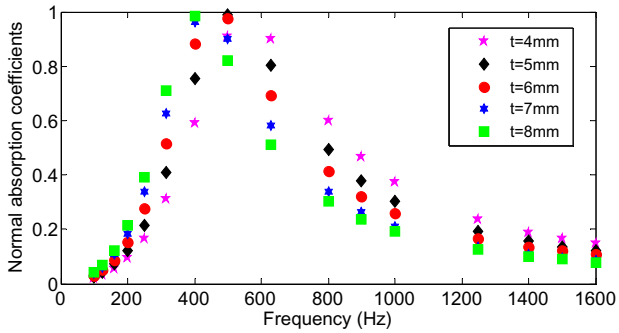

Fig. 11—Normal incidence absorption coefficient of Set 3 MPP absorbers.

bandwidth has increasing trend. One possible reason is that the porosity increases greatly as the hole inlet diameter increases, which will lead to a significant decrease in the acoustic mass of the MPP, while a relative small decrease in the acoustic resistance. Figure 11 (set 3) shows that the maximum absorption coefficient is shifted to low frequency as the panel thickness increases, with no change in the absorption bandwidth. One likely reason is that the increase of the panel thickness just increases the acoustic mass of the MPPs, but has little influence on their acoustic resistance. The findings can help to strike a balance between the maximum absorption coefficient and the absorption bandwidth according to the actual demand, and if the maximum absorption coefficient is desired, the hole outlet diameter should be relative large and the hole inlet diameter should be relative small. Conversely, if broad absorption bandwidth is needed, the hole outlet diameter should be relative small and the hole inlet diameter should be relative large. Furthermore, if the noise is at the low frequency range, the panel thickness is probably suggested to be large.

6 CONCLUSION

In this paper, a finite element model (FEM) is built to numerically study the acoustic properties of MPPs with tapered holes, which is difficult for traditional analytical models. Firstly, the finite element model of a single hole needs to be established to obtain its specific acoustic impedance, and then the normal incidence acoustic impedance of an MPP can be calculated. Compared with the traditional analytical models, the finite element model is more simple and effective in handling MPPs with irregular-shaped holes and thus has more flexible applications. The validity of the FEM is experimentally verified, and based on the FEM, a series of numerical parametric studies on the normal absorption performance of MPPs with tapered holes is conducted. Results show that the absorption performance of MPPs with tapered holes is mostly affected by both the hole inlet diameter and the hole outlet diameters. When the hole outlet diameter gradually increases or the hole inlet diameter of the front side decreases, the maximum absorption coefficient increases, but the absorption bandwidth decreases. In the meantime, panel thickness just influences the resonance frequency corresponding to the maximum absorption coefficient and the resonance frequency is shifted to low frequency when the panel thickness increases and vice versa. These findings are meaningful in the design of MPPs with tapered holes.

In future work it would be useful to confirm the assumption that the end corrections do not need to be accounted for in the FEM calculations for thick MPPs. Moreover, the optimization method and effective manufacturing method of MPPs with tapered holes to realize a high absorption absorber with broader bandwidth should be expected.

7 REFERENCES

1. D.Y. Maa, "Theory and design of micro-perforated panel sound-absorbing constructions", *Sci. Sinica*, **18**(1), 55–71, (1975).
2. D.Y. Maa, "Potential of microperforated panel absorber", *J. Acoust. Soc. Am.*, **104**(5), 2861–2866, (1997), doi:10.1121/1.423870.
3. H.V. Fuchs and X. Zha, "Micro-perforated structures as sound absorbers — a review and outlook", *Acta Acustica*, **92**(1), 139–166, (2006).
4. M.Q. Wu, "Micro-perforated panels for duct silencing", *Noise Control Engr. J.*, **45**(2), 69–77, (1997), doi:10.3397/1.2828428.
5. F. Asdrubali and G. Pispola, "Properties of transparent sound absorbing panels for use in noise barriers", *J. Acoust. Soc. Am.*, **121**(1), 214–221 (2007), doi:10.1121/1.2395916.
6. D. Takahashi and M. Tanaka, "Flexural vibration of perforated plates and porous elastic materials under acoustic loading", *J. Acoust. Soc. Am.*, **112**(4), 1456–1464, (2002), doi:10.1121/1.1497624.
7. Y.Y. Lee, E.W.M. Lee and C.F. Ng, "Sound absorption of a finite flexible micro-perforated panel backed by an air cavity", *J. Sound Vibr.*, **287**(1), 227–243, (2005), doi:10.1016/j.jsv.2004.11.024.
8. Y.Y. Lee, H.Y. Sun, and X. Guo, "Effects of the panel and Helmholtz resonances on a micro-perforated panel absorber", *Int. J. of Appl. Math and Mech.*, **4**, 49–54, (2005).
9. Y. Lee and E.W.M. Lee, "Widening the sound absorption bandwidths of flexible micro-perforated curved absorbers using structural and acoustic resonances", *Int. J. Mech Sci*, **49**(8), 925–934, (2007), doi:10.1016/j.ijmecsci.2007.01.008.
10. D.Y. Maa, "Microperforated-panel wideband absorber", *Noise Control Engr. J.*, **29**(3), 77–84, (1987), doi:10.3397/1.2827694.
11. I. Mada Miasa and Masaaki Okuka, "Theoretical and experimental study on sound absorption of a multi-leaf microperforated panel", *Acoustic Science & Technology*, **1**(1), 63–72, (2007).
12. D.H. Lee and Y.P. Kwon, "Estimation of the absorption performance of multiple layer perforated panel systems by transfer matrix method", *J. Sound Vibr.*, **278**(4), 847–860, (2004), doi:10.1016/j.jsv.2003.10.017.
13. K. Sakagami, "A pilot study on improving the absorptivity of a thick micro perforated panel absorber", *Appl. Acoust.*, **69**(2), 179–182, (2008), doi:10.1016/j.apacoust.2006.09.008.

14. D.Y. Maa, "Theory of micro-slit absorbers", *Acta Acustica*, **25**(6), 481–485, (2000).
15. J.D. Achenbach, "3-D reflection and transmission of sound by an array of rods", *J. Sound Vibr.*, **125**(3), 463–476, (1988), doi:10.1016/0022-460X(88)90254-4.
16. J. Liu and D.W. Herrin, "Enhancing micro-perforated panel attenuation by partitioning the adjoining cavity", *Appl. Acoust.*, **71**(2), 120–127, (2010), doi:10.1016/j.apacoust.2009.07.016.
17. V. Easwaran and M.L. Munjal, "Analysis of reflection characteristics of a normal incidence plane wave on resonant absorbers: a finite element approach", *J. Acoust. Soc. Am.*, **93**(3), 1308–1318, (1993), doi:10.1121/1.405416.
18. O. Onen, "Design of a single layer micro-perforated sound absorber by finite element analysis", *Appl. Acoust.*, **71**(1), 79–85, (2010), doi:10.1016/j.apacoust.2009.07.012.
19. N. Atalla and F. Sgard, "Modeling of perforated plates and screens using rigid frame porous models", *J. Sound Vibr.*, **303**(1), 195–208, 2007, doi:10.1016/j.jsv.2007.01.012.
20. A. Viswanathan and J.S. Bolton, "Study of the effect of grazing flow on the performance of microperforated and perforated panels", *NoiseCon13*, (2013).
21. K. Hou and J.S. Bolton, "Finite element models for microperforated materials", *InterNoise09*, (2009).
22. R.T. Randeberg, "Perforated Panel Absorbers with Viscous Energy Dissipation Enhanced by Orifice Design", PhD Thesis, Trondheim, (2000).
23. J.S. Bolton and N.N. Kim, "Use of CFD to calculate the dynamic resistive end end correction for microperforated materials", *Acoustics Australia*, **38**(3), 134–144, (2010).
24. T. Herdtle, J.S. Bolton, N.N. Kim, J.H. Alexander and R.W. Gerdes, "Transfer impedance of microperforated materials with tapered holes", *J. Acoust. Soc. Am.*, **134**(6), 4752–4762, (2013), doi:10.1121/1.4824968.
25. L. Rayleigh, *Theory of Sound*, Macmillan, New York, (1945).
26. I.B. Crandall, *Theory of Vibrating Systems and Sound*, Van Notrand, New York, (1926).
27. S. Allam and M. Abom, "Noise control for cooling fans on heavy vehicles", *Noise Control Engr. J.*, **60**(6), 707–715, (2012), doi:10.3397/1.3701042.
28. S. Allam and M. Abom, "Fan noise control using microperforated baffle silencers", *J. Vib. Acoust.*, **136**(3), 031017, (2014).
29. W.M. Beltman, P.J.M. van der Hoogt, R.M.E.J. Spiering and H. Tijdeman, "Implementation and experimental validation of a new viscothermal acoustic finite element for acousto-elastic problems", *J. Sound Vibr.*, **216**(1), 159–185, 1998, doi:10.1006/jsvi.1998.1708.
30. D.Y. Maa, "Microperforated panel at high sound intensity", *Acta Acustica*, **21**(1), 10–14, (1996).
31. ISO 10534-1, "Acoustics — Determination of Sound Absorption Coefficients and Impedance In Impedance Tubes — Part 1: Method Using Standing Wave Ratio", (1998).